Stability of the staging structure of charge-transfer complexes showing a neutral–ionic transition

Takako Iizuka-Sakano, Tohru Kawamoto, Yukihiro Shimoi, and Shuji Abe
Nanotechnology Research Institute (NRI) and Research Consortium for Synthetic Nano-Function Materials Project (SYNAF), National Institute of Advanced Industrial Science and Technology (AIST), 1-1-1 Umezono, Tsukuba, Ibaraki 305-8568, Japan
(Received 23 February 2004; published 25 August 2004)

The stability of staging states has been investigated for mixed-stack charge-transfer complexes, TMB-TCNQ [(3,3′,5,5′)-tetramethylbenzidine-(7,7,8,8)tetracyanoquinodimethane], DMTTF-CA (dimethyltetrathiafulvalene-*p*-chloranil), and TTF-CA (tetrathiafulvalene-*p*-chloranil) crystals, by the calculation of their electrostatic energies considering intramolecular charge distributions. The staging state, a superstructure consisting of an alternative sequence of the ionic and neutral domains, is supposed to be advantageous for reducing the repulsive interaction between neighboring chains in the ionic phase. However, our calculations indicate that the electrostatic interchain interaction is attractive, implying that the staging state is disadvantageous. Nevertheless, a staging state can be marginally stabilized around the neutral–ionic transition in TMB-TCNQ although the energy difference between the staging state and the uniform ionic state is quite small.

DOI: 10.1103/PhysRevB.70.085111 PACS number(s): 71.15.Nc, 73.21.Cd

I. INTRODUCTION

A phase transition takes place in some quasi-one-dimensional charge-transfer (CT) organic crystals which are formed by mixed stacks of alternating donor (D) and acceptor (A) molecules: the neutral (N)–ionic (I) transition.[1] It manifests itself by a change of the degree of CT, often followed by lattice dimerization in the I phase, and has been observed by applying pressure,[1] decreasing temperature,[2] and photo-irradiation.[3] It is accompanied with such intriguing properties as a sharp discontinuous increase of dc conductivity,[4] negative-resistance effects,[5] and an unusual dielectric response.[6] These properties are related to the mobile defects such as charge and spin solitons and NI domain walls.[7–9] The NI transition has also drawn attention from the viewpoint of controlling such interesting properties.

There is an interesting possibility of "staging" due to frustrated interstack Coulomb interaction in the I phase. In the crystal structure of the CT complexes, the same kinds of molecules may be located as nearest neighbors of an interstack direction, and such an alignment seems to give rise to Coulomb repulsion between them, which may destabilize the I phase. Hubbard and Torrance have theoretically proposed a model called the staging structure which is a superlattice that has N layers inserted between I layers so as to reduce the interchain repulsion.[10] Bruinsma *et al.* have argued that the ionization of the lattice may occur progressively via multiple, periodic long-range ordering between N and I layers, within an infinite stepped sequence of first-order transitions (devil's staircase).[11]

The staging state would be observed as a coexistent state of the N and I layers which are arrayed with a periodicity longer than a lattice constant. The coexistence of N and I states has been observed in (3,3′,5,5′)-tetramethylbenzidine-(7,7,8,8)tetracyanoquinodimethane (TMB-TCNQ),[12,13] dimethyltetrathiafulvalene-*p*-chloranil (DMTTF-CA),[14] and tetrathiafulvalene-*p*-chloranil (TTF-CA)[2] which are typical complexes driving the NI transition. Collet *et al.* have reported that the coexistent state in DMTTF-CA is a staging state with dimerization.[15] The details are presented in the next section.

The proposal for staging structure by Hubbard and Torrance[10] and the related theoretical works[11,16] are based on the replacement of each planar molecule by a single site at its center of mass, which we call a point *molecule* approximation. This approximation reveals that an electrostatic interaction is repulsive between the chains in the direction in which the same kinds of molecules are located. However, we recently demonstrated that the electrostatic interchain interaction was *attractive* in TTF-CA[17] by taking account of the charge distribution within the molecules (a point *atom* approximation). This result is not consistent with the prerequisite for the original staging model. Therefore, one question arises: is it possible for a staging state to appear in any complex?

In the present paper, we theoretically investigate electrostatic energies of staging states in TMB-TCNQ, DMTTF-CA, and TTF-CA crystals using the point atom approximation. The method used to obtain the charge density distributions of a molecule at a fractional degree of CT is an *ab initio* quantum chemical method.[18] The details are given in Sec. III. The obtained charge distributions of TMB, TCNQ, and DMTTF molecules are presented in the Appendix. In Sec. IV, electrostatic energies are calculated for various modifications of the crystal structure at the I phase of the crystals. The results show that the electrostatic interactions of interchain directions are attractive for both TMB-TCNQ and DMTTF-CA as well as TTF-CA. This seems to be disadvantageous for stable staging states. In Sec. V, an energy gain of a staging state against a uniform ionic state is presented. The energy gain is quite small but the sign depends on the complex. This indicates that a staging state can be stable even in attractive electrostatic interaction. It is found that a staging state is marginally stabilized in TMB-TCNQ around the NI transition. We also investigate the effect of lattice dimerization on the stability of a staging state in

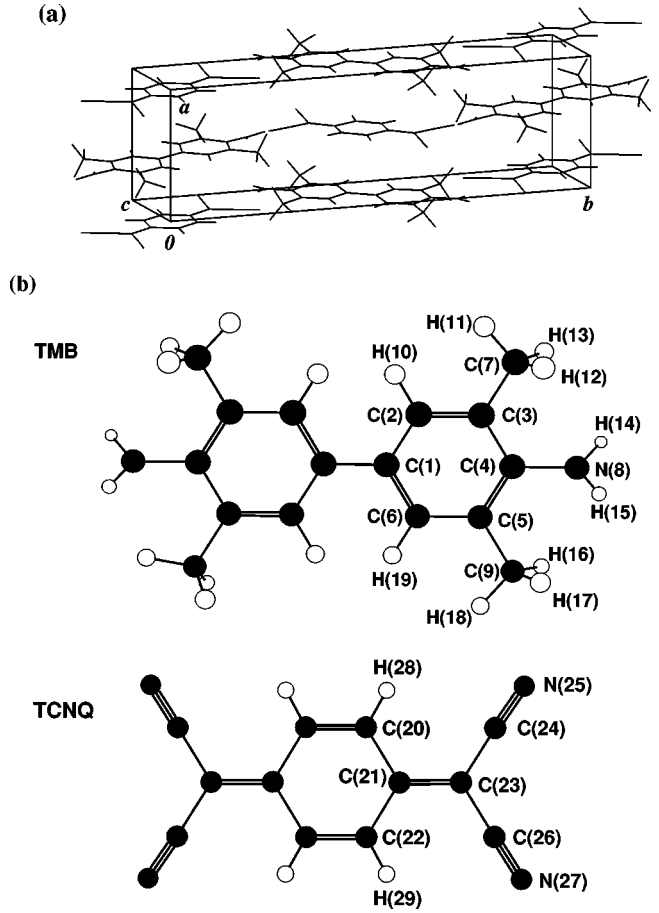

FIG. 1. (a) Crystal structure of TMB–TCNQ in the high-temperature phase. (b) Molecules of TMB and TCNQ with the atoms labeled.

DMTTF-CA.[15] We show that the dimerization effect is very small. In Sec. VI we present concluding remarks.

II. COMPLEXES AND THEIR CRYSTAL STRUCTURES

In this section, we present the crystal structures of TMB-TCNQ, DMTTF-CA, and TTF-CA, and the experimental results of their staging and coexisting states.

TMB-TCNQ is one of the typical complexes showing the NI transition where the degree of CT changes from $\rho \sim 0.6$ in the N phase to $\rho \sim 0.7$ in the I phase at $T_{NI}=200$ K at ambient pressure.[12,13] Iwasa *et al.* observed the coexistence of the N and I states in the pressure range from 6 kbar to 20 kbar[13] at room temperature. They proposed that this corresponds to the staging state, although not confirmed yet.

Figure 1(a) is the crystal structure of TMB-TCNQ determined by the x-ray diffraction measurements at room temperature in the N phase.[19] It is monoclinic, $P2_1/n$, and the lattice constants are a (stacking axis) =6.727 Å, $b=21.90$ Å, $c=8.12$ Å, and $\beta=104.14°$. There are two equivalent stacks in a unit cell. Each molecule has inversion symmetry.

DMTTF-CA is another complex in which the temperature-induced NI transition takes place at $T_{NI} \sim 65$ K. The degree of CT is $\rho \sim 0.3$ in the high-temperature N phase

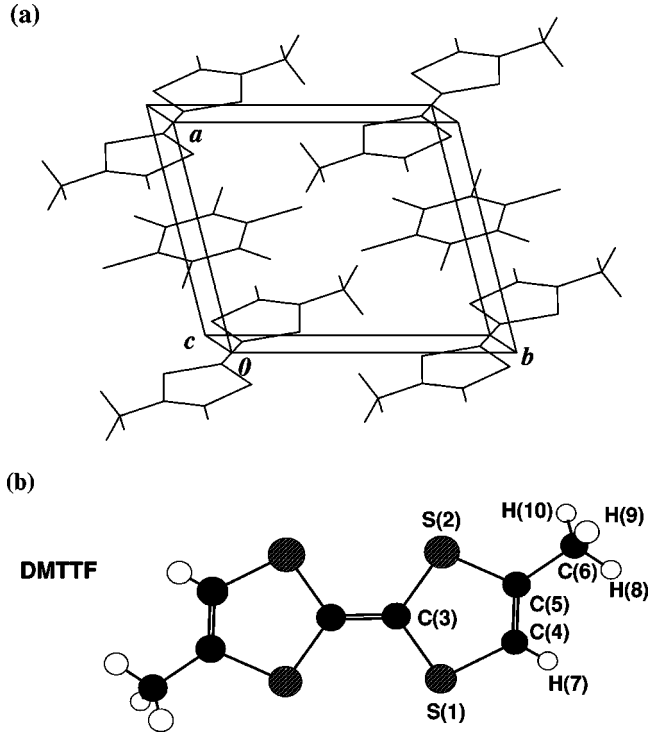

FIG. 2. (a) Crystal structure of DMTTF-CA in the high-temperature phase. (b) DMTTF molecule with the atoms labeled. The CA molecule is shown in Fig. 3(b).

and $\rho \sim 0.6-0.7$ (Ref. 14) or 0.4–0.5 (Ref. 20) in the low-temperature phase. Aoki *et al.* have presented that N and I states coexist in the low-temperature phase, using polarized visible reflection spectroscopy.[14] Collet *et al.* have reported that this phase is a staging state with dimerization in both the N and I regions, based on their x-ray diffraction experiments.[15] On the other hand, Horiuchi *et al.* have concluded by infrared molecular-vibrational spectroscopy that it is a homogeneous I state.[20]

Figure 2(a) is the crystal structure of DMTTF-CA determined by the x-ray diffraction measurements by Collet *et al.*[15] at 75 K in the N phase. It is triclinic, $P\bar{1}$, and the lattice constants are a (stacking axis) =7.121 Å, $b=7.5864$ Å, $c=8.476$ Å, $\alpha=95.87°$, $\beta=104.07°$, and $\gamma=90.92°$. There is only one stack in a unit cell and the molecules maintain inversion symmetry.

The low-temperature phase of DMTTF-CA, is noncentrosymmetric triclinic $P1$ with the c parameter doubled from that of the high-temperature phase, with alternating N and I chains along the c axis.[15] The N chain is less dimerized than the I chain: the center-to-center distances between the nearest neighbor DMTTF and CA molecules in the N chain are 3.490 Å and 3.609 Å, while those in the I chain are 3.458 Å and 3.641 Å at 40 K.

TTF-CA also exhibits a temperature-induced NI transition at $T_{NI}=80$ K (Ref. 2) with a change in the degree of CT from $\rho \sim 0.3$ in the N phase to $\rho \sim 0.7$ in the I phase.[21] Though its coexisting state has been observed in a certain range of temperature and pressure,[7,22] it is not understood as a staging state but as merely a mixed state of N and I states.[22,23]

Figure 3(a) is the crystal structure of TTF-CA determined by neutron-scattering measurements at 90 K in the N

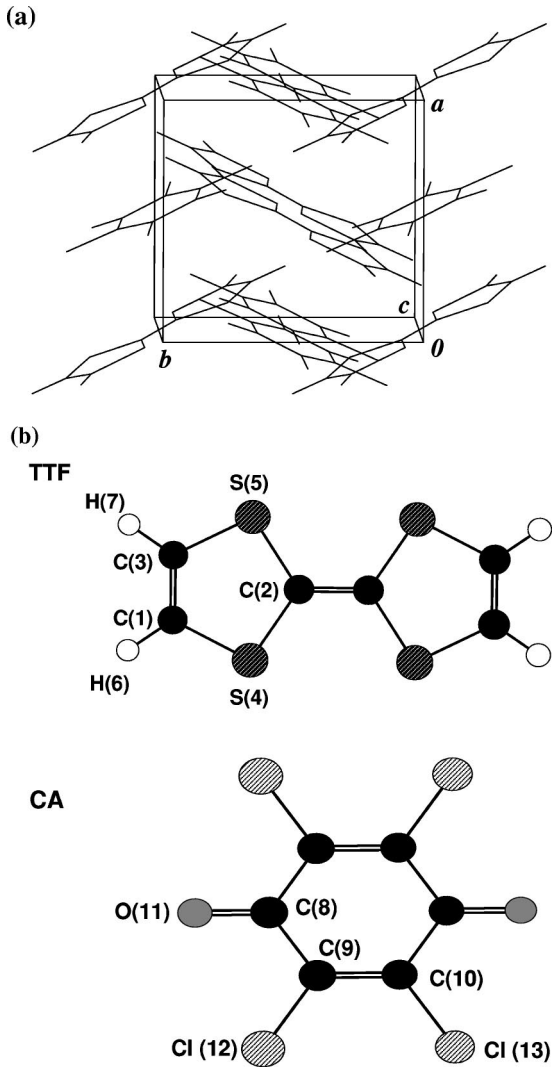

FIG. 3. (a) Crystal structure of TTF-CA in the high-temperature phase. (b) Molecules of TTF and CA with the atoms labeled.

phase.[24] It is monoclinic, $P2_1/n$, and the lattice constants are a (stacking axis)=7.22 Å, b=7.59 Å, c=14.49 Å, and β=99.1°. There are two equivalent stacks in a unit cell. Each molecule has inversion symmetry.

III. INTRAMOLECULAR CHARGE DISTRIBUTIONS

We calculated the charge distribution on a molecule using an *ab initio* quantum chemical method.[18] Mulliken charges on an isolated molecule were used as an intramolecular charge distribution. They were calculated for both neutral and monovalent states using the restricted and unrestricted Hartree-Fock methods, respectively. We used the basis function set of 6-31G*. The obtained charge distributions in TMB, TCNQ, DMTTF, TTF, and CA molecules are tabulated for both neutral and monovalent states in the Appendix.

In the actual CT complexes, the degree of CT is fractional in either the N or I phase as mentioned in Sec. II. We denote the charge on atom i in an isolated molecule for neutral and monovalent states by $q_i^{(0)}$ and $q_i^{(1)}$, respectively. The charge density q_i in a CT state with a fractional degree of CT, ρ, is estimated by a linear interpolation between the charge densities $q_i^{(0)}$ and $q_i^{(1)}$ as shown by

$$q_i = q_i^{(0)} + \rho \delta q_i, \tag{1}$$

where $\delta q_i = q_i^{(1)} - q_i^{(0)}$. Note that they have large polarization charge even in the completely neutral state.

IV. INTERCHAIN INTERACTION

In this section, we investigate whether the electrostatic interaction between neighboring chains is attractive or repulsive in TMB-TCNQ and DMTTF-CA as well as TTF-CA by the point atom approximation. Intermolecular electrostatic energy E_M in the crystals was calculated with the Ewald method.

Figure 4 shows variations in electrostatic energy E_M against uniaxial deformations along the interchain directions. The intramolecular atomic coordinates and the charge density distributions were fixed against the deformations. The variations in the energy E_M were calculated for both the point atom [Figs. 4(a)–4(c)] and point molecule [Figs. 4(d)–4(f)] approximations. (a) and (d) are for TMB-TCNQ at ρ=0.69, (b) and (e) are for DMTTF-CA at ρ=0.65, and (c) and (f) are for TTF-CA at ρ=0.7. In the figure, "a," "b," or "c" represents the direction of the uniaxial deformation of the lattice. The results for the b axis in TTF-CA have already been reported in Ref. 17. Note that the ordinates of these figures have different scales between (a)–(c) and (d)–(f).

As shown in Fig. 4, E_M increases against the compression to the c axis in (d), that to the b axis in (e), and that to the b axis in (f) with the point *molecule* approximation. This means that the electrostatic interactions between chains are repulsive to the respective directions of the crystals with this approximation. This supports the proposal of the staging state by Hubbard and Torrance. This is reasonable since those axes have shorter lattice constants than the others along the interchain directions in the crystals. In DMTTF-CA, the lines b and c in Fig. 4(e) show different tendencies in spite of the similar values of lattice constants in the b and c axes. This may arise from the large deviation of the unit cell angle β=104.07°, which reduces the electrostatic interaction between chains in the c axis.

However, E_M decreases markedly against the compression in all of the crystals with the point *atom* approximation. This indicates that the electrostatic interactions between the chains are attractive. The results similar to those previously shown for TTF-CA are also obtained for TMB-TCNQ and DMTTF-CA. Therefore, it is demonstrated that the electrostatic interaction is attractive between the chains in all of these complexes. In the following, we will analyze the origin of the attractive interaction in TMB-TCNQ and DMTTF-CA based on their molecular arrangement and the charge density distribution.

First, we examine the interchain interaction along the c axis in TMB-TCNQ. Figure 5(a) shows molecular alignment of TMB-TCNQ within the ac plane and electrostatic energies between the molecules at ρ=0.69 (I phase) within the point atom approximation. The electrostatic energy between TMB

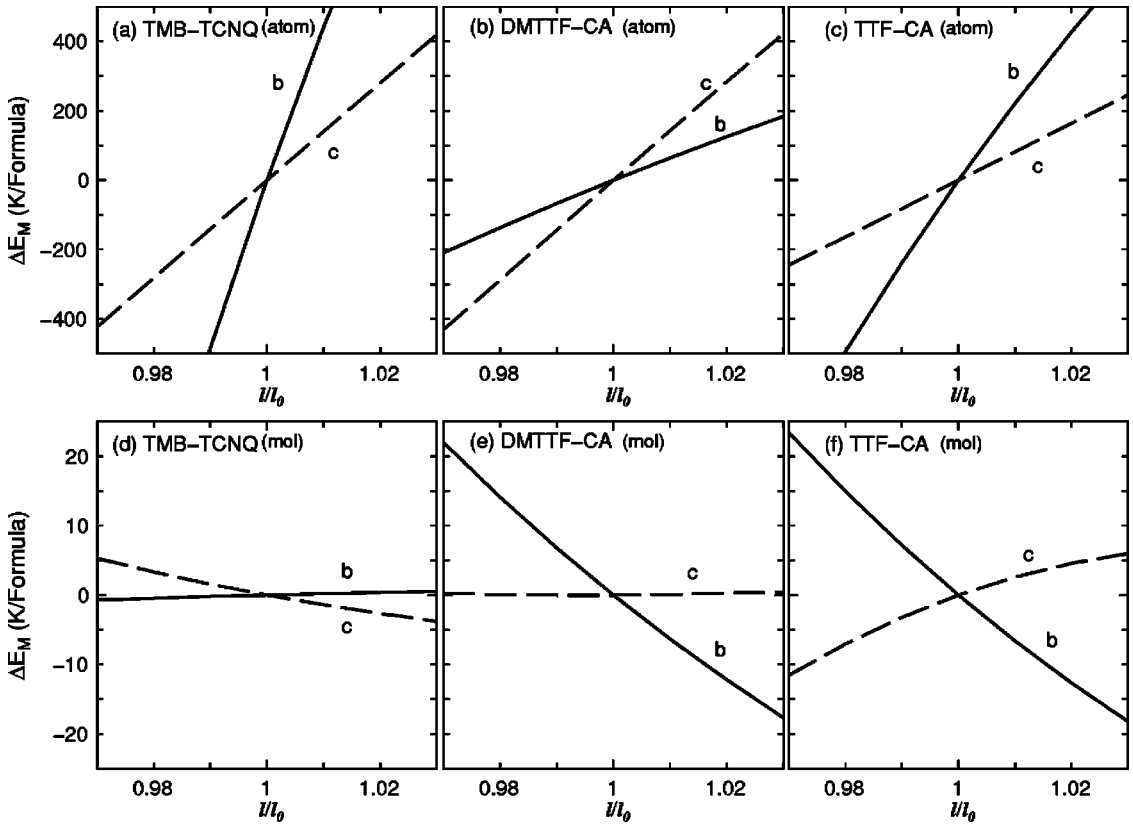

FIG. 4. Shifts of E_M due to the variation of each lattice constant (l) along the interchain direction from that (l_0) observed for TMB -TCNQ [(a) and (d)], DMTTF-CA [(b) and (e)], and TTF-CA [(c) and (f)]. While (a)–(c) were obtained by the point atom approximation, (d)–(f) were obtained by the point molecule approximation. In the figure, "a," "b" or "c" represents the direction of the uniaxial deformation of the lattice. Note that the ordinates of these figures have different scales between (a)–(c) and (d)–(f).

and TCNQ molecules along the $\boldsymbol{a}/2+\boldsymbol{c}$ direction is −0.78 eV. It is outweighed by that between TMB molecules along the c axis (0.91 eV) but dominates that between TCNQ molecules along the same direction (0.56 eV). Since the attractive interaction from a TCNQ molecule, $(-0.78\ \text{eV}+0.56\ \text{eV})\times 2=-0.44$ eV, is larger than the repulsive one from a TMB molecule, $(0.91\ \text{eV}-0.78\ \text{eV})\times 2=0.26$ eV, the total of the electrostatic interactions between the chains becomes attractive along the c axis.

Second, we discuss the interchain interaction along the b axis. Figure 5(b) shows the molecular alignment of TMB-TCNQ within the bc plane and electrostatic energies between the molecules at $\rho=0.69$ (I phase). The hydrogen–nitrogen intermolecular contacts, C–H(TMB)···N(TCNQ) marked by dotted lines in Fig. 5(b), have larger interactions than the others in this complex. Their interactions become larger to the uniaxial deformation along the b axis. This is the reason why the attractive interaction is larger in point atom approximation than that in point molecule one. Note that the origin of the attractive interaction between chains is quite different in between TMB-TCNQ and TTF-CA. The hydrogen–nitrogen contacts in TMB-TCNQ are in the bc plane. However, the hydrogen bondings C–H(TTF)···O(CA) in TTF-CA are in the ab plane,[25] which is the plane containing the stacking axis.

Next, we investigate the interchain interaction along the b axis in DMTTF-CA. Figure 6 shows the molecular alignment of the DMTTF-CA crystal within the (a) ab and (b) ac planes. Electrostatic energies between molecules at $\rho=0.65$ (low-temperature phase) are also shown. Black indicates that the charge is positive and white indicates a negative charge. Each atomic charge is depicted by its radius. From Fig. 6(a), it is found that the electrostatic energy between the nearest DMTTF and CA molecules aligned along $\boldsymbol{a}/2+\boldsymbol{b}$ direction is −0.79 eV and this attractive energy overcomes the repulsive ones between DMTTF molecules (0.73 eV) along the b axis. Electrostatic energy between DMTTF and other molecules in the nearest stacks along the b axis is $(-0.79\ \text{eV}+0.73\ \text{eV})\times 2=-0.12$ eV and that between CA and other molecules is $(-0.79\ \text{eV}+0.80\ \text{eV})\times 2=0.02$ eV. Therefore the electrostatic interaction between chains along the b axis becomes predominantly attractive.

Finally, we examine the interchain interaction along the c axis. In the ac plane, electrostatic energy between DMTTF and CA molecules aligned along the $\boldsymbol{a}/2+\boldsymbol{c}$ direction is −0.87 eV (attractive), as shown in Fig. 6(b). It dominates repulsive interactions between CA molecules (0.73 eV) along the c axis. Though the electrostatic energy between DMTTF and other molecules in the nearest stacks along the c axis almost vanishes $(-0.87+0.87=0\ \text{eV})$, that between CA and other molecules is $(-0.87\ \text{eV}+0.73\ \text{eV})\times 2=-0.28$ eV. Therefore the interaction between the chains along the c axis also becomes predominantly attractive.

These attractive interactions mainly come from the C–H(DMTTF)···O(CA) hydrogen–oxygen intermolecular con-

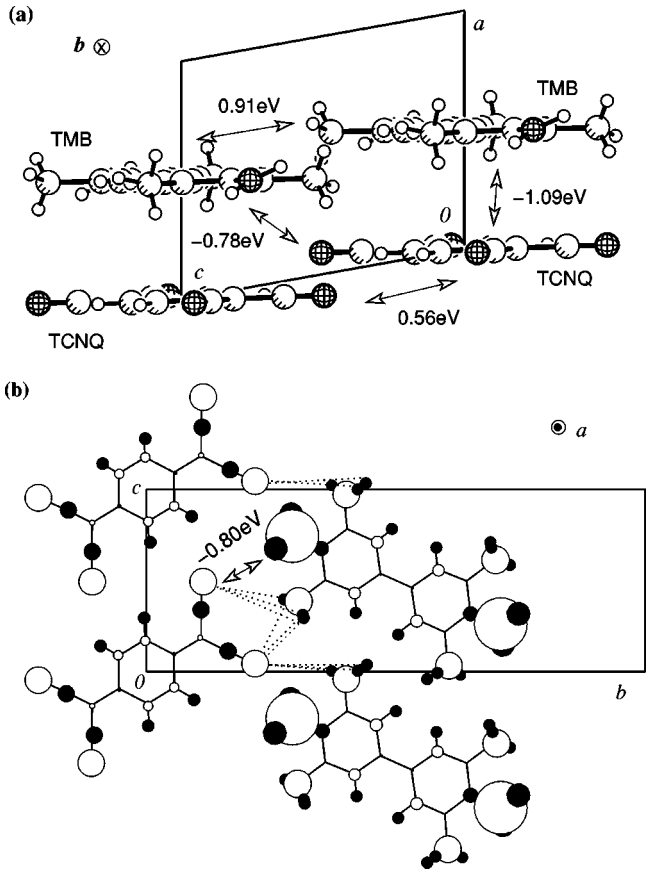

FIG. 5. Molecular alignment of TMB-TCNQ within the (a) *ac* and (b) *bc* planes, and electrostatic energies between the molecules. In (b), each atomic charge is depicted by its radius (black for positive, white for negative). The hydrogen–nitrogen intermolecular contacts, C–H(TMB)···N(TCNQ), are marked by dotted lines.

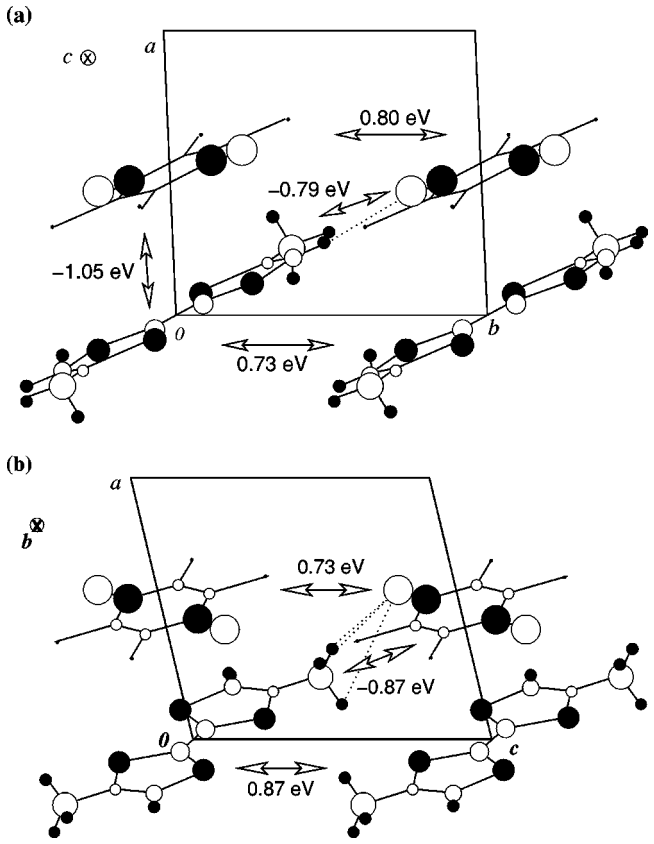

FIG. 6. Molecular alignment of DMTTF-CA within the (a) *ab* and (b) *ac* planes and electrostatic energies between the molecules. Each atomic charge is depicted by its radius. Black indicates the positive charge, white indicates negative.

tact shown by a dotted line in Fig. 6(a), which is similar to the case of TTF-CA.[26] Other strong hydrogen–oxygen interactions, C−H(methyl in DMTTF) ···O(CA), are shown by dotted lines in Fig. 6(b).

V. STAGING STRUCTURE

The attractive interchain interaction is opposite to the original idea of the staging model. Nevertheless, we found that a staging state can be stable even in such a situation. In this section, we confirm this by comparing the energy of the staging state with that in the uniform I state.[27]

Among many possible kinds of staging structures, we assume particular structures in which the regions of the I and N states are in the ratio of 1:1 as shown in Fig. 7: (a) is the structure proposed for TMB-TCNQ by Iwasa *et al.*,[13] and (b) is the one reported for DMTTF-CA by Collet *et al.*[15] For TTF-CA, we assume a pattern similar to that in TMB-TCNQ [Fig. 7(c)].

We denote the degree of CT in the regions marked I and N in the figures as ρ_{I} and ρ_{N}, respectively, whose values are assumed to be the same as in uniform I and N states.

We separate the total energy of the system into the electrostatic energy E_{M} and the other contributions E_{ex},

$$E_{\mathrm{total}}^{(k)} = E_{\mathrm{M}}^{(k)} + E_{\mathrm{ex}}^{(k)}, \tag{2}$$

where k=S, I, and N specify the staging, ionic, and neutral states, respectively. The electrostatic energy in the staging state is expressed as

$$E_{\mathrm{M}}^{(\mathrm{S})} = \sum_{\langle i,j\rangle \in I} q_i^{\mathrm{I}} q_j^{\mathrm{I}}/r_{ij} + \sum_{\langle i,j\rangle \in N} q_i^{\mathrm{N}} q_j^{\mathrm{N}}/r_{ij} + \sum_{i\in I, j\in N} q_i^{\mathrm{I}} q_j^{\mathrm{N}}/r_{ij}. \tag{3}$$

Here, q_i^{I} and q_i^{N}, respectively, denote the charge distribution of atom i in the I and N regions, calculated with Eq. (1). In the uniform I (N) state, the electrostatic energy is given by replacing $q^{\mathrm{N}}(q^{\mathrm{I}})$ by $q^{\mathrm{I}}(q^{\mathrm{N}})$ in Eq. (3). The energy $E_{\mathrm{ex}}^{(k)}$ comes, for example, from the effective ionization potential and the elastic energy due to the lattice dimerization.

Since we consider a situation around the NI transitions, we assume that the uniform I and N states are degenerate, $E_{\mathrm{total}}^{(\mathrm{I})} = E_{\mathrm{total}}^{(\mathrm{N})}$, which is rationalized in the vicinity of the transition point. The energy gain $\Delta\epsilon$ of the staging state based on the uniform states is given as

$$\Delta\epsilon = \{E_{\mathrm{total}}^{(\mathrm{I})} - E_{\mathrm{total}}^{(\mathrm{S})}\} = \{E_{\mathrm{total}}^{(\mathrm{I})} + E_{\mathrm{total}}^{(\mathrm{N})} - 2E_{\mathrm{total}}^{(\mathrm{S})}\}/2 = \Delta E_{\mathrm{M}} + \Delta E_{\mathrm{ex}}, \tag{4}$$

where ΔE_{M} and ΔE_{ex} are energy gains of a staging state, respectively, for E_{M} and E_{ex}. We assume that $E_{\mathrm{ex}}^{(k)}$ is proportional to the numbers of molecules in the I and N regions,

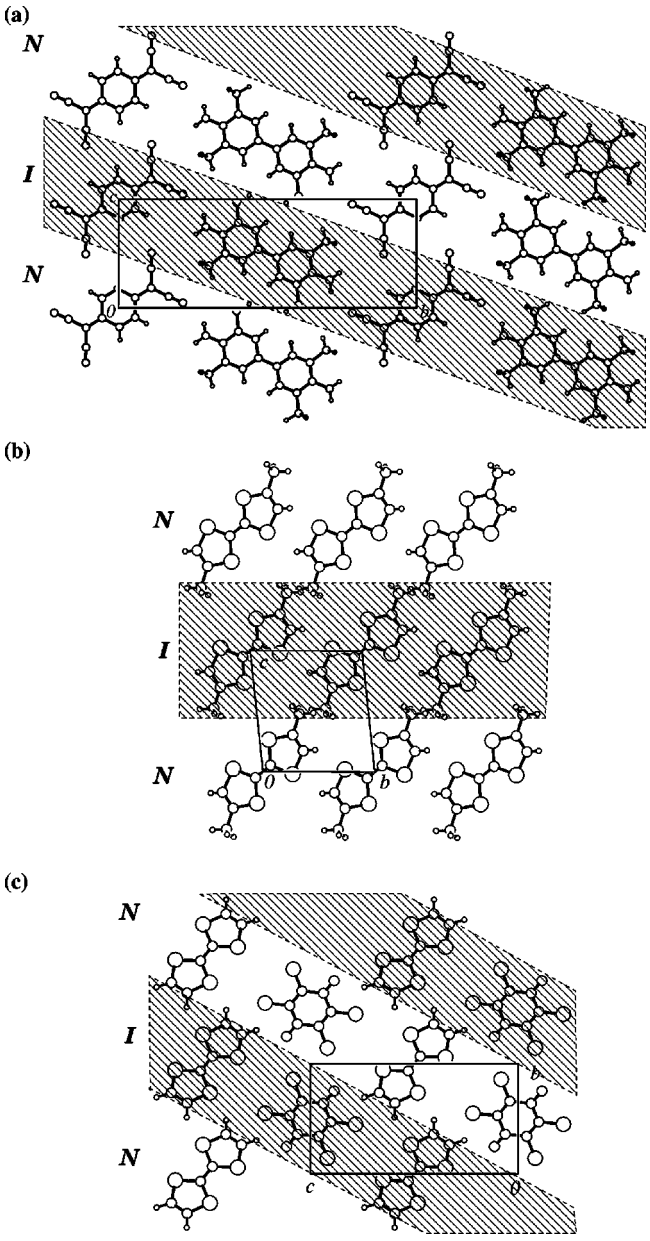

FIG. 7. Molecular arrangements in (a) TMB-TCNQ, (b) DMTTF-CA, and (c) TTF-CA perpendicular to the stacking axis. Hatched and unhatched parts indicate the ionic (I) and neutral (N) regions proposed for TMB-TCNQ by Iwasa *et al.* (Ref. 13) and reported for DMTTF-CA by Collet *et al.* (Ref. 15). For TTF-CA, we assumed the pattern (c) in our discussion.

resulting in the fact that the energy gains of E_{ex} are written as

$$\Delta E_{\mathrm{ex}} = \{E_{\mathrm{ex}}^{(\mathrm{I})} + E_{\mathrm{ex}}^{(\mathrm{N})} - 2E_{\mathrm{ex}}^{(\mathrm{S})}\}/2 = 0. \tag{5}$$

Therefore, $\Delta\epsilon$ is obtained only by ΔE_{M},

$$\Delta\epsilon = \Delta E_{\mathrm{M}} = \{E_{\mathrm{M}}^{(\mathrm{I})} + E_{\mathrm{M}}^{(\mathrm{N})} - 2E_{\mathrm{M}}^{(\mathrm{S})}\}/2. \tag{6}$$

For a while, we fix the atomic positions to those observed in the N phase. Then,

TABLE I. Calculated $\Delta\epsilon$ for the staging states of Fig. 7 for DMTTF-CA, TMB-TCNQ, and TTF-CA with the crystal structure of the neutral phase.

	TMB-TCNQ	DMTTF-CA	TTF-CA
$\Delta\epsilon$ (eV)	0.0023	−0.0266	−0.0247

$$\begin{aligned}\Delta\epsilon &= \sum_{i\in I, j\in N}\{q_i^{\mathrm{I}}q_j^{\mathrm{I}}/2r_{ij} + q_i^{\mathrm{N}}q_j^{\mathrm{N}}/2r_{ij} - q_i^{\mathrm{I}}q_j^{\mathrm{N}}/r_{ij}\} \\ &+ \left\{\sum_{\langle i,j\rangle\in N} - \sum_{\langle i,j\rangle\in I}\right\}q_i^{\mathrm{I}}q_j^{\mathrm{I}}/2r_{ij} + \left\{\sum_{\langle i,j\rangle\in N} - \sum_{\langle i,j\rangle\in I}\right\}q_i^{\mathrm{N}}q_j^{\mathrm{N}}/2r_{ij} \\ &= \frac{1}{2}\left(\sum_{i\in I, j\in N}\frac{\delta q_i \delta q_j}{r_{ij}}\right)\Delta\rho^2, \end{aligned} \tag{7}$$

where δq_i is defined as $q_i^{(1)} - q_i^{(0)}$ as shown in Eq. (1). The value $\Delta\rho$ is defined as $\rho_{\mathrm{I}} - \rho_{\mathrm{N}}$. The second line in Eq. (7) vanishes because the I and N domains are identical with respect to their geometry. Defining α_{NI} as

$$\alpha_{\mathrm{NI}} = -\sum_{i\in I, j\in N}\frac{\delta q_i \delta q_j}{r_{ij}}, \tag{8}$$

the energy gain $\Delta\epsilon$ is reduced to

$$\Delta\epsilon = -\alpha_{\mathrm{NI}}\Delta\rho^2/2. \tag{9}$$

Note that the sign of α_{NI} is independent of the electrostatic interaction between the chains in the case of considering charge distributions in a molecule.

Table I is the calculated values of $\Delta\epsilon$ with $\Delta\rho = 1$ for each complex using Eqs. (8) and (9). Here we use the patterns of staging shown in Fig. 7, which are proposed or observed in each complex as mentioned above. The values of $\Delta\epsilon$ are 0.0023 eV for TMB-TCNQ, and −0.0266 eV and −0.0247 eV for DMTTF-CA and TTF-CA, respectively, suggesting that the staging state is slightly stable in TMB-TCNQ. In DMTTF-CA, there is another set of structural data obtained by Nogami *et al.* with the x-ray diffrac-

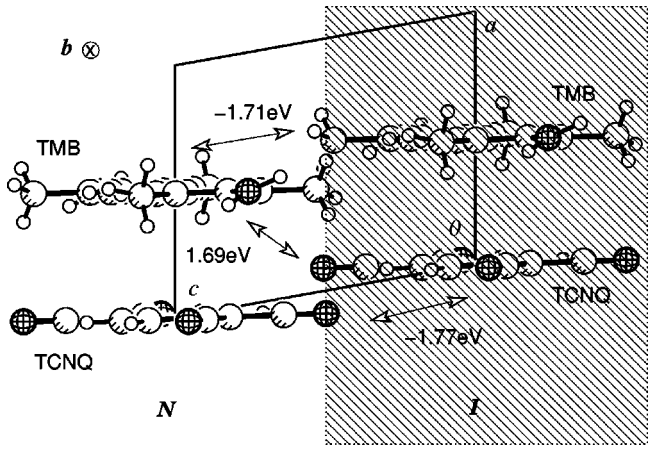

FIG. 8. Molecular arrangement within the *ac* plane of the TMB-TCNQ crystal in the staging state. The values represent the contribution to α_{NI} from a pair of molecules.

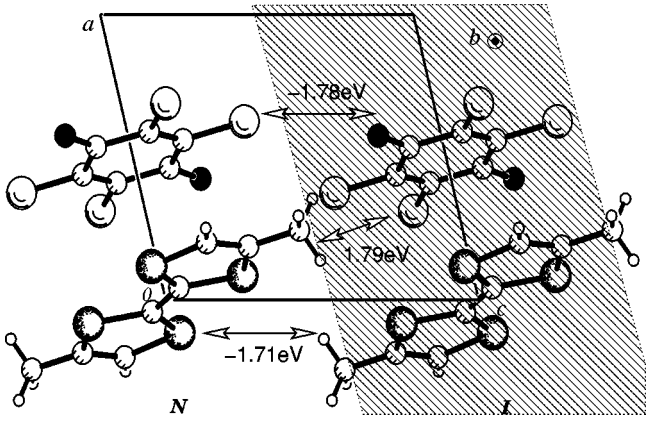

FIG. 9. Molecular arrangement within the *ac* plane of DMTTF-CA crystal in the staging state. It shows the contribution to α_{NI} from a pair of molecules.

tion experiment.[28] We calculated the energy gain of staging also by using the data. Obtained results are almost the same.

We discuss $\Delta\epsilon$ of the complexes in detail. Figure 8 shows the molecular arrangement of a TMB-TCNQ crystal in the staging state and the contribution to α_{NI} from each pair of molecules. The contribution is −1.71 eV from the TMB pair, −1.77 eV from the TCNQ pair, and 1.69 eV from the pair of TMB and TCNQ along the $\boldsymbol{a}/2+\boldsymbol{c}$ direction. The sum of the contributions from the neighbor pairs is $(-1.71\ \mathrm{eV}+1.69\ \mathrm{eV})\times 2=-0.04$ eV of a TMB molecule and $(-1.77\ \mathrm{eV}+1.69\ \mathrm{eV})\times 2=-0.16$ eV from a TCNQ molecule. These are the main reasons of the positive value of $\Delta\epsilon$, advantageous to the staging stage.

The case of DMTTF-CA is shown in Fig. 9. The contribution is −1.71 eV from the DMTTF pair, −1.78 eV from the CA pair, and 1.79 eV from the pair of DMTTF and CA across the regions. The sum of the contribution from the neighbor pairs is $(-1.71\ \mathrm{eV}+1.79\ \mathrm{eV})\times 2=0.16$ eV of a DMTTF molecule and $(-1.78\ \mathrm{eV}+1.79\ \mathrm{eV})\times 2=0.02$ eV from a CA molecule. These are the main reasons of the negative value of $\Delta\epsilon$, disadvantageous to the staging stage.

In the case of TTF-CA, it is difficult to explain why $\Delta\epsilon$ is negative as is shown in Table I. Each molecule is tilted to the stacking axis in TTF-CA. The directions are different in each stacking chain in a unit cell. There are many pairs of molecules whose contributions to $\Delta\epsilon$ are largely positive or largely negative. Therefore, the sign of $\Delta\epsilon$ is determined by the delicate balance of all the contributions. This is the reason for the difficulty.

TABLE II. Electrostatic energies of DMTTF-CA in the I, N, and staging states at some lattice dimerization d in the I phase and I region of the staging state, where the degree of dimerization d is the change of the intermolecular distance of the ionized DMTTF-CA pair normalized by the lattice constant along the stacking axis.

d	0.00	0.01	0.02	0.03
$\Delta\epsilon$ (eV)	−0.0266	−0.0266	−0.0265	−0.0264
$E_{\mathrm{M}}^{(\mathrm{I})}$ (eV)	−3.6316	−3.6323	−3.6342	−3.6374
$E_{\mathrm{M}}^{(\mathrm{N})}$ (eV)	−0.2610	−0.2610	−0.2610	−0.2610
$E_{\mathrm{M}}^{(\mathrm{S})}$ (eV)	−1.9197	−1.9200	−1.9211	−1.9228

Finally we discuss the effect of the lattice dimerization along the stacking axis in DMTTF-CA. In the presence of dimerization, $\Delta\epsilon$ is not simplified as Eqs. (8) and (9) but should be calculated directly from Eq. (6). Table II summarizes the values of $\Delta\epsilon$ and $E_{\mathrm{M}}^{(\mathrm{k})}$ (k=I, N, and S) calculated for several degrees of dimerization. We assumed that only ionic DMTTF molecules are shifted along the stacking axis because the displacements of the other molecules are comparatively small in the observed dimerization.[15] The degree of dimerization d is defined as the change of the intermolecular distance of the ionized DMTTF-CA pair normalized by the lattice constant along the stacking axis. Its observed value is 0.014.[15] With increasing d, the electrostatic energies $E_{\mathrm{M}}^{(\mathrm{I})}$ and $E_{\mathrm{M}}^{(\mathrm{S})}$ decrease, but the resultant energy gain of the staging state $\Delta\epsilon$ changes very little, as shown in Table II. The change of $E_{\mathrm{M}}^{(\mathrm{I})}$ due to the dimerization is small as discussed in Ref. 24 within dipolar energy for TTF-CA.

The decrease in $E_{\mathrm{M}}^{(\mathrm{I})}$ and $E_{\mathrm{M}}^{(\mathrm{S})}$ is mainly due to the energy gain within the chains. On the other hand, $\Delta\epsilon$ is determined by the energies of interchain molecular pairs. The intrachain dimerization only slightly changes their distances, and consequently their electrostatic energies. Therefore, it is reasonable that dimerization has little effect on $\Delta\epsilon$.

In the above discussion, we assumed that the atomic positions and lattice constants were fixed, neglecting the effects

TABLE III. Charge density on each atom of TTF and CA molecules (Ref. 17) in the neutral and monovalent states. Their differences are also shown.

Atom	Neutral	Monovalent	Difference	Atom	Neutral	Monovalent	Difference
TTF							
C(1)	−0.37	−0.37	0.00	S(5)	0.32	0.49	−0.18
C(2)	−0.38	−0.36	−0.02	H(6)	0.24	0.31	−0.06
C(3)	−0.37	−0.37	0.00	H(7)	0.24	0.31	−0.06
S(4)	0.31	0.49	−0.18				
CA							
Cl(8)	0.13	0.00	0.13	C(11)	0.60	0.52	0.08
Cl(9)	0.13	0.00	0.13	C(12)	−0.19	−0.21	0.02
O(10)	−0.48	−0.60	0.12	C(13)	−0.20	−0.22	0.02

TABLE IV. Charge density on each atom of TMB and TCNQ molecules in the neutral and monovalent states. Their differences are also shown.

Atom	Neutral	Monovalent	Difference	Atom	Neutral	Monovalent	Difference
TMB							
C(1)	0.01	0.04	−0.03	H(11)	0.19	0.21	−0.02
C(2)	−0.24	−0.21	−0.03	H(12)	0.18	0.21	−0.03
C(3)	−0.02	−0.01	−0.01	H(13)	0.17	0.20	−0.03
C(4)	0.23	0.26	−0.03	H(14)	0.38	0.41	−0.03
C(5)	−0.00	0.01	−0.01	H(15)	0.38	0.41	−0.03
C(6)	−0.23	−0.20	−0.03	H(16)	0.18	0.20	−0.03
C(7)	−0.48	−0.48	−0.00	H(17)	0.19	0.22	−0.03
N(8)	−0.96	−0.91	−0.05	H(18)	0.18	0.20	−0.03
C(9)	−0.50	−0.50	0.00	H(19)	0.17	0.22	−0.04
H(19)	0.17	0.21	−0.04				
TCNQ							
C(20)	−0.15	−0.19	0.03	N(25)	−0.43	−0.51	0.09
C(21)	0.06	0.05	0.01	C(26)	0.30	0.29	0.02
C(22)	−0.16	−0.19	0.03	N(27)	−0.42	−0.51	0.09
C(23)	−0.00	−0.13	0.12	H(28)	0.25	0.20	0.05
C(24)	0.30	0.29	0.02	H(29)	0.25	0.20	0.05

of entropy and volume changes. These effects would make the quantitative comparisons of the stability among the three phases delicate since both of the energy difference and many of its contributions are small or of same order as the thermal energy at the transition temperature. It will be important to calculate free energies taking into account entropy effects which are reported in Refs. 22 and 29.

VI. CONCLUSION

In summary, we studied the electrostatic energies of TMB-TCNQ, DMTTF-CA, and TTF-CA using the point atom approximation. They are attractive between the chains in each complex. This is opposite to the original idea of the staging. Nevertheless, we showed that a staging state can be stable even in such a situation by comparing the energies at the uniform I state with those at the staging state. We calculated the energy gain of the staging state for the complexes. A staging state can be marginally stabilized around the neutral–ionic transition in TMB-TCNQ although the energy difference between the staging state and the uniform ionic state is quite small. We also found that the energy gain only slightly depends on the lattice dimerization in DMTTF-CA.

ACKNOWLEDGMENTS

The authors thank Dr. Horiuchi for giving unpublished data of the crystal structure for TMB-TCNQ and fruitful discussions. They also thank Professor Nogami for giving unpublished data of the crystal structure for DMTTF-CA. The calculations have been performed on IBM SR6000 and Hitachi SR8000 at the Tsukuba Advanced Computer Center (TACC) of National Institute of Advanced Industrial Science and Technology (AIST). This work was partly supported by NEDO under the Nanotechnology Materials Program.

APPENDIX: CALCULATED CHARGE DISTRIBUTION

Charge density distributions on TTF and CA molecules have already been obtained by Kawamoto *et al.*[17] as shown

TABLE V. Charge density on each atom of DMTTF molecules in the neutral and monovalent states. Their differences are also shown.

Atom	Neutral	Monovalent	Difference	Atom	Neutral	Monovalent	Difference
DMTTF							
S(1)	0.31	0.47	−0.16	C(6)	−0.46	−0.47	−0.01
S(2)	0.29	0.48	−0.19	H(7)	0.15	0.19	−0.04
C(3)	−0.38	−0.36	−0.02	H(8)	0.20	0.22	−0.02
C(4)	−0.28	−0.27	−0.01	H(9)	0.19	0.23	−0.04
C(5)	−0.21	−0.22	0.01	H(10)	0.20	0.22	−0.02

in Table III. Figure 3(a) is the crystal structure determined at 90 K.[24] The crystal is in the N phase and the molecules have inversion symmetry.

Table IV lists the obtained charges on each atom of TMB and TCNQ molecules, which are labeled in Fig. 1(b). The molecular structures extracted from the crystal structures determined by the x-ray diffraction measurements at room temperature in the N phase[19] are used in the calculation. These molecules maintain the inversion symmetry.

Table V lists the obtained charges on each atom of DMTTF molecule which are labeled in Fig. 2(b). For the CA molecule, the same distribution is used as that of TTF-CA. There is little difference in the obtained charge distributions in spite of the fact that there is a slight difference in the molecular structure of the CA molecules between TTF-CA and DMTTF-CA crystals. The crystal structure of DMTTF-CA determined at 75 K in the N phase[15] is used.

[1] J. B. Torrance, J. E. Vazquez, J. J. Mayerle, and V. Y. Lee, Phys. Rev. Lett. **46**, 253 (1981).

[2] J. B. Torrance, A. Girlando, J. J. Mayerle, J. I. Crowley, V. Y. Lee, P. Batail, and S. J. LaPlaca, Phys. Rev. Lett. **47**, 1747 (1981).

[3] S. Koshihara, Y. Tokura, T. Mitani, G. Saito, and T. Koda, Phys. Rev. B **42**, 6853 (1990).

[4] T. Mitani, G. Saito, Y. Tokura, and T. Koda, Phys. Rev. Lett. **53**, 842 (1984).

[5] Y. Tokura, H. Okamoto, T. Koda, T. Mitani, and G. Saito, Phys. Rev. B **38**, 2215 (1988).

[6] H. Okamoto, T. Mitani, Y. Tokura, S. Koshihara, T. Komatsu, Y. Iwasa, T. Koda, and G. Saito, Phys. Rev. B **43**, 8224 (1991).

[7] T. Mitani, Y. Kaneko, S. Tanuma, Y. Tokura, T. Koda, and G. Saito, Phys. Rev. B **35**, 427 (1987).

[8] N. Nagaosa, J. Phys. Soc. Jpn. **55**, 2754 (1986).

[9] N. Nagaosa, Solid State Commun. **57**, 179 (1986).

[10] J. Hubbard and J. B. Torrance, Phys. Rev. Lett. **47**, 1750 (1981).

[11] R. Bruinsma, P. Bak, and J. B. Torrance, Phys. Rev. B **27**, 456 (1983).

[12] Y. Iwasa, T. Koda, Y. Tokura, A. Kobayashi, N. Iwasawa, and G. Saito, Phys. Rev. B **42**, 2374 (1990).

[13] Y. Iwasa, N. Watanabe, T. Koda, and G. Saito, Phys. Rev. B **47**, 2920 (1993).

[14] S. Aoki, T. Nakayama, and A. Miura, Phys. Rev. B **48**, 626 (1993).

[15] E. Collet, M. Buron-Le Cointe, M. H. Lemée-Cailleau, H. Cailleau, L. Toupet, M. Meven, S. Mattauch, G. Heger, and N. Karl, Phys. Rev. B **63**, 054105 (2001).

[16] L. M. Floría, P. Quémerais, and S. Aubry, J. Phys.: Condens. Matter **4**, 5921 (1992).

[17] T. Kawamoto, T. Iizuka-Sakano, Y. Shimoi, and S. Abe, Phys. Rev. B **64**, 205107 (2001).

[18] M. J. Frisch, G. W. Trucks, H. B. Schlegel *et al.*, GAUSSIAN 98, Revision A.9 (Gaussian Inc., Pittsburgh, PA, 1988).

[19] S. Horiuchi, unpublished (2001).

[20] S. Horiuchi, Y. Okimoto, R. Kumai, and Y. Tokura, J. Am. Chem. Soc. **123**, 665 (2001).

[21] C. S. Jacobsen and J. B. Torrance, J. Chem. Phys. **78**, 112 (1983).

[22] M. Buron-Le Cointe, M. H. Lemée-Cailleau, H. Cailleau, B. Toudic, A. Moréac, F. Moussa, C. Ayache, and N. Karl, Phys. Rev. B **68**, 064103 (2003).

[23] K. Takaoka, Y. Kaneko, H. Okamoto, Y. Tokura, T. Koda, T. Mitani, and G. Saito, Phys. Rev. B **36**, 3884 (1987).

[24] M. Le Cointe, M. H. Lemée-Cailleau, H. Cailleau, B. Toudic, L. Toupet, G. Heger, F. Moussa, P. Schweiss, K. H. Kraft, and N. Karl, Phys. Rev. B **51**, 3374 (1995).

[25] P. Batail, S. J. LaPlaca, J. J. Mayerle, and J. B. Torrance, J. Am. Chem. Soc. **103**, 951 (1981).

[26] V. Oison, C. Katan, and C. Koenig, J. Phys. Chem. A **105**, 4300 (2001).

[27] T. Iizuka-Sakano, T. Kawaoto, Y. Shimoi, and S. Abe, Phase Transitions **75**, 831 (2002).

[28] Y. Nogami, unpublished (2000).

[29] T. Kawamura, Y. Miyazaki, and M. Sorai, Chem. Phys. Lett. **273**, 435 (1997).